Neutron-diffraction study of bulk amorphous $Al_{32}Ge_{68}$ alloy

A. I. Kolesnikov
Institute of Solid State Physics, Russian Academy of Sciences, 142432 Chernogolovka, Moscow District, Russia and Department of Physics, UMIST, P.O. Box 88, Manchester, M60 1QD, United Kingdom

U. Dahlborg and M. Calvo-Dahlborg
LSG2M, CNRS UMR 7584, Ecole des Mines, Parc de Saurupt, 54042 Nancy Cedex, France

O. I. Barkalov* and E. G. Ponyatovsky
Institute of Solid State Physics, Russian Academy of Sciences, 142432 Chernogolovka, Moscow District, Russia

W. S. Howells
ISIS Facility, Rutherford Appleton Laboratory, Chilton, Didcot, Oxon, OX11 0QX, United Kingdom

A. I. Harkunov
Institute of Solid State Physics, Russian Academy of Sciences, 142432 Chernogolovka, Moscow District, Russia
(Received 26 April 1999; revised manuscript received 5 August 1999)

A neutron-diffraction study was carried out at 100 K on a bulk amorphous $Al_{32}Ge_{68}$ alloy produced by the thermobaric technique. Fourier transformation of the measured structure factor and reverse Monte Carlo simulations have been performed to obtain a total radial distribution function and three-dimensional atom configurations. It was found that the effective coordination number ($n=4.5$) is appreciably higher than 4, the characteristic for tetrahedral coordination. The partial atom-atom correlations obtained are analyzed and the results indicate a well-defined covalent bonding between Ge atoms and rather broad distribution for Al-Ge and Al-Al nearest neighbors. [S0163-1829(99)02142-6]

I. INTRODUCTION

As was shown in the set of previous studies,[1–4] the metastable high-pressure crystalline phases in some binary systems of *B* elements, recovered at low temperature to ambient pressure, undergo transformation to the amorphous state in the course of heating. The structure of the resulting bulk amorphous alloys was studied by neutron diffraction[5–8] and transmission electron microscopy[9,10] for Zn-Sb, Ga-Sb, and Al-Ge systems. The composition of the amorphous alloy of the Zn-Sb system is $Zn_{41}Sb_{59}$ (here and below in atomic percents, at. %) which is close to that for the equilibrium equiatomic ZnSb.[11] In the case of the Ga-Sb system, amorphous alloys can be obtained in the composition range 47.4–52.5 at. % of Sb, thus including the composition of the equiatomic low-pressure phase.[11] The closeness in composition of crystalline low-pressure phases and the amorphous alloys formed gives rise to a similarity in the short-range order observed for these phases.[5–8]

At normal pressure, the Al-Ge system is a binary system with the eutectic point at 424 °C and about 30 at. % of Ge.[11] Both components have limited solid solubility and there are no intermediate equilibrium phases in Al-Ge alloys. However, it is possible to produce various metastable crystalline phases by rapid solidification of the melts or by fast annealing of thin amorphous films.[12–15] The equilibrium phase diagram of the Al-Ge system changes by applying high pressure. The Ge solubility in Al increases up to 18 at. % at 7 GPa, and two intermediate phases are observed at higher pressures for Ge compositions of 68 and 45–50 at. % (Ref. 16). It is possible to obtain these phases in a metastable state at ambient pressure by means of thermobaric quenching.[2,17] The recovered high-pressure γ phase with 68 at. % Ge has a simple hexagonal structure and it transforms to the amorphous state on heating to 130 °C at normal pressure.[10] Preliminary measurements of the electrical properties have shown that our amorphous product is a semiconductor.

It is of considerable interest to investigate what changes are induced by a significantly large amount of trivalent Al in the tetrahedral network of amorphous tetravalent Ge. Below we present the results of a neutron-diffraction investigation of the bulk amorphous alloy of $Al_{32}Ge_{68}$ composition.

II. EXPERIMENTAL DETAILS

The first step in the sample production was to produce a single-phase sample of the high-pressure γ phase by submitting a crystalline powder of the $Al_{32}Ge_{68}$ alloy to 9-GPa pressure at 320 °C for about 24 h. This was followed by cooling under pressure to liquid-nitrogen temperature and a release of the pressure to atmospheric. The final sample tablets were in the form of discs, 7 mm in diameter and about 2 mm thick, and the amorphous state was produced by heating (20 °C/min) to 130 °C. After production each tablet was checked for crystalline inclusions by x-ray diffraction and stored in liquid-nitrogen Dewar.

The neutron-diffraction experiment was carried out on the LAD diffractometer at the ISIS pulsed neutron source, Rutherford Appleton Laboratory, U.K.[18] The data were collected in a wide range of neutron momentum transfer *Q*, from 0.5 to

35 Å^{-1}. The ISIS pulsed neutron source produces neutrons with a spread of energies (or wavelengths) that gives an opportunity to measure the intensity of neutrons scattered from the sample into fixed angle detectors as a function of time-of-flight. The data obtained can be directly transformed to momentum-transfer spectra. The time-of-flight technique makes it possible to measure a complete diffraction pattern over the entire momentum-transfer range simultaneously.

The pellets of the amorphous $Al_{32}Ge_{68}$ sample studied were packed into a cylindrical vanadium container of 8.0-mm inner diameter. The measurements were carried out using a standard ''orange'' cryostat kept at a temperature of 100 K. The experiment consisted of four measurements: with the sample in the container, with the empty container, without the sample and container (the background measurement), and with a vanadium rod. The vanadium neutron cross section is almost entirely incoherent, and the latter measurement was used for normalization of the sample data. The measured time-of-flight spectra were transformed to structure factors $S(Q)$ by using the ATLAS correction program package.[19] The total radial distribution function, $G(r)$, was calculated by the Fourier transformation of the $S(Q)$ spectra (with $Q_{\max}=35$ Å^{-1}) using the standard transformation techniques,

$$G(r)=1+\frac{1}{2\pi^2\rho_0 r}\int_0^{Q_{\max}} Q[S(Q)-1]\sin(Qr)\frac{\sin\alpha(Q)}{\alpha(Q)}dQ, \tag{1}$$

where ρ_0 is the average atomic density ($\rho_0=0.0458$ atom/Å^3, which corresponds to 4.41 ± 0.06 g/cm^3) and the modification function $\alpha(Q)$ is given by $\alpha(Q)=\pi Q/Q_{\max}$.

III. NEUTRON-DIFFRACTION RESULTS

The aluminum and germanium nuclei are predominantly coherent scatterers of neutrons. The corresponding scattering cross sections are $\sigma_{\mathrm{Al}}^{\mathrm{coh}}=1.495$ b and $\sigma_{\mathrm{Ge}}^{\mathrm{coh}}=8.42$ b. As the sample is a two-component alloy it is essential to know the magnitude of the different structural correlations that make up the total scattering intensity. The contribution of the partial structure factors $S_{ij}(Q)$ to the corresponding total $S(Q)$ is given by the expression:

$$S(Q)=\sum_{i,j}\sqrt{x_i x_j \sigma_i^{\mathrm{coh}}\sigma_j^{\mathrm{coh}}}S_{ij}(Q). \tag{2}$$

The sum is over all different types of atom pairs (i,j), x_i is the concentration of atom of type i, and a partial structure factor $S_{ij}(Q)$ is defined in Ref. 20 as

$$S_{ij}(Q)=\delta_{ij}+4\pi\rho_0\sqrt{x_i x_j}\int_0^{\infty}[G(r)-1]\frac{\sin(Qr)}{Qr}r^2dr. \tag{3}$$

The relative weights of the oscillating part of Al-Al, Al-Ge, and Ge-Ge partial structure factors of the total $S(Q)$ are 0.03, 0.16, and 0.81, respectively.

Figures 1 and 2 show the experimental structure factor $S(Q)$ obtained and the corresponding total radial distribution function $G(r)$ for the amorphous $Al_{32}Ge_{68}$ sample. The weight coefficients above indicate that the curves in the figures are mainly represented by Ge-Ge and Al-Ge atomic correlations, while the Al-Al correlations are hardly discernible.

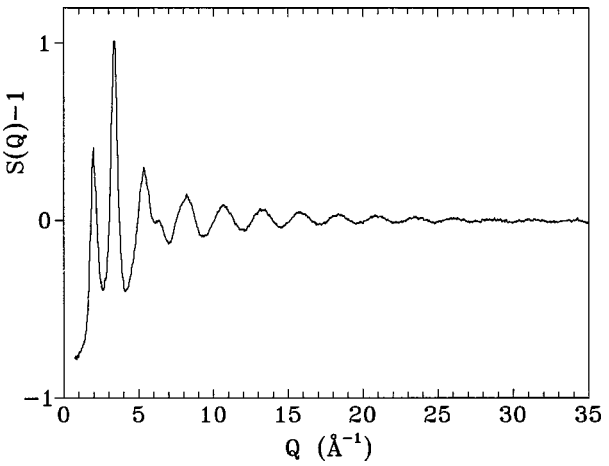

FIG. 1. Total experimental structure factor for amorphous $Al_{32}Ge_{68}$ alloy at 100 K.

The experimental data in Fig. 1 clearly show that the sample studied was a good quality amorphous material. No diffraction peaks, characteristic of crystalline inclusions, were observed in the diffraction pattern recorded at the largest diffraction angle (150°), which has the best resolution (0.5% $\Delta Q/Q$). The maximum of the first and the second peaks in the $S(Q)$ curve are at about 1.96 and 3.35 Å^{-1} and oscillations are clearly seen up to 30 Å^{-1}.

The $G(r)$ function of amorphous $Al_{32}Ge_{68}$, shown in Fig. 2, exhibits a distinct and narrow first peak at $r_1=2.478$ Å. There is no sign of a prepeak indicating some kind of chemical ordering. The first peak is very well separated from the remainder of $G(r)$ and this, in principle, makes it possible to accurately calculate the coordination number n, i.e., the average number of atoms in the nearest-neighbor shell. Performing the appropriate integration of the total radial distribution function up to 3 Å the value $n=4.5\pm0.1$ is obtained. This is significantly larger than 4, which indicates that a well-developed tetrahedral bonding network does not exist in amorphous $Al_{32}Ge_{68}$. It should though be noted that the ratio of the positions of the second and the first peaks in $G(r)$, $r_2/r_1\approx4.03/2.48\approx1.625$ is close to the tetrahedral value 1.633. However, in order to understand the structure of

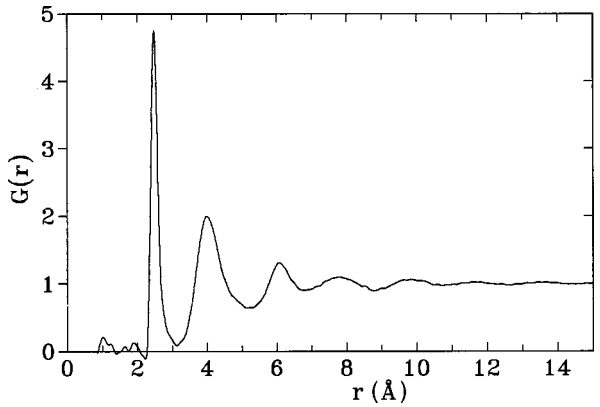

FIG. 2. The total radial distribution function, $G(r)$, for amorphous $Al_{32}Ge_{68}$ obtained by Fourier transformation of $S(Q)$.

TABLE I. Parameters obtained from a fit of the first peak of $G(r)$ for amorphous $Al_{32}Ge_{68}$ alloy by a sum of three Gaussian functions.

Gaussian peak number	Position of peak (Å)	Width of peak (Å)	Coordination number
1	2.467±0.006	0.132	2.93
2	2.60±0.08	0.20	1.02
3	2.80±0.15	0.33	0.54

amorphous $Al_{32}Ge_{68}$ it is important to realize that the first peak exhibits a very distinct shoulder above 2.6 Å. For a quantitative description of the first peak it was fitted by a least-squares method with a sum of three Gaussians. The parameters of the fit are given in Table I. The origin of this shoulder which, together with a tail, persists up to 3.1 Å can be explained as follows: from the composition of the alloy it can be evaluated that the probability for an Al atom to have another one or even two Al atoms as nearest neighbors is relatively high because the average number of Al atoms near Al atom is about $0.32\times4.5=1.44$. If it is assumed that Al and Ge atoms do not form any covalent bonds, it may, from a geometrical point of view, be easily anticipated that around an Al-Al dimer (or trimer) there will be a larger number of Ge atoms than would have been the case if only covalent bonds with tetrahedral coordination were possible. This would result in a coordination number for noncovalently bonded Al-Ge pairs greater than 4. Accordingly, the shoulder and the tail for the right-hand side of the first peak in the $G(r)$ ranging up to 3.1 Å may correspond to Al-Ge and Al-Al nearest-neighbor arrangements.

IV. REVERSE MONTE CARLO SIMULATIONS

To elucidate the partial atom-atom correlations in the amorphous alloy studied a reverse Monte Carlo (RMC) method was applied. This technique is described thoroughly in Refs. 21–23 and it has been already used, with differing degrees of success, for simulations of tetrahedrally coordinated amorphous Si (Refs. 24 and 25), Ge (Refs. 25 and 26), and C (Refs. 25, 27–29). In the present RMC calculations 1000 atoms of aluminum and germanium were randomly generated in the cubic box of size of 27.95 Å with proper concentration and average atomic density. Closest atom-atom distance constraints were applied to prevent atoms from being closer than 2.25 Å for any of Al-Al, Al-Ge, and Ge-Ge pairs; the use of a larger value in the RMC simulations resulted in an abrupt vertical cutoff on the left-hand side of the first peak of the partial $G(r)$ functions (the details of the RMC technique could be found in Refs. 21–23). The structure factor $S_{\rm cal}(Q)$ was calculated for this atomic arrangement, assuming periodic boundary conditions. The criterion relevant to the agreement between the calculated and experimental structure factors was calculated by using the equation:

$$\chi^2=\sum_{i=1}^{m}\left[S_{\rm cal}(Q_i)-S_{\rm exp}(Q_i)\right]^2/\sigma(Q_i)^2, \qquad (4)$$

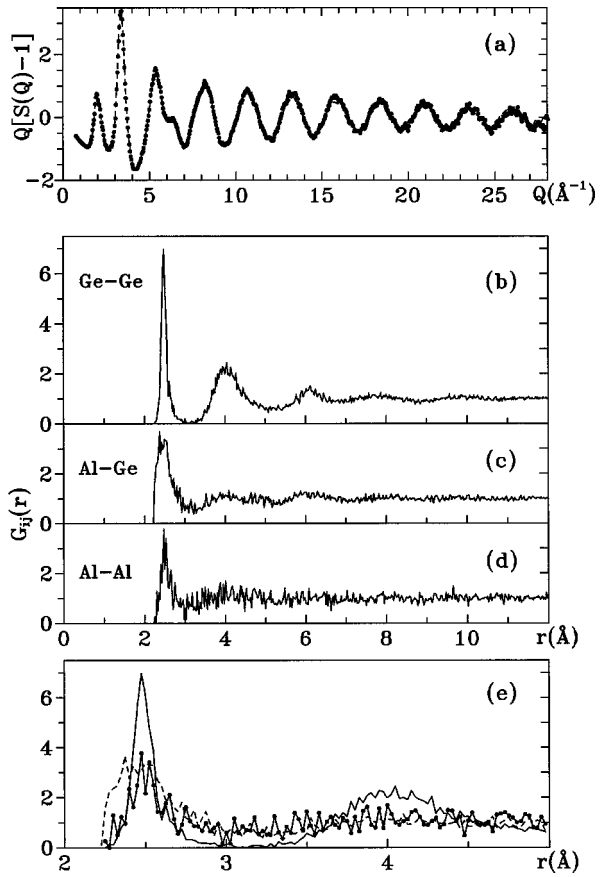

FIG. 3. (a) Total experimental (points) and RMC fit (dashed line) reduced structure factors $Q[S(Q)-1]$ for amorphous $Al_{32}Ge_{68}$. Partial radial distribution functions for amorphous $Al_{32}Ge_{68}$ obtained by RMC modeling: (b) $G_{\rm GeGe}(r)$, (c) $G_{\rm AlGe}(r)$, (d) $G_{\rm AlAl}(r)$; (e) the partial $G_{ij}(r)$plotted in a larger r scale for Al-Al, Al-Ge, and Ge-Ge pairs by solid line with points, dashed line, and solid line, respectively.

where the sum is over all m experimental data points, each having an error $\sigma(Q_i)$. A randomly chosen atom was then moved randomly (with a maximum step of 0.05 Å, and obeying the constraints conditions). If the new calculated χ^2 was smaller than the previous one, this atomic move was accepted, otherwise the move was accepted with probability $\exp[-(\chi^2_{\rm new}-\chi^2_{\rm old})/2]$. Another atom was then randomly chosen to move and the above procedure was repeated until convergence was reached, i.e., when the obtained three-dimensional atomic configuration produces a calculated structure factor, which satisfactorily describes the experimental data.

As can be seen from Fig. 3(a) the agreement between the calculated and experimental structure factors is excellent (reduced structure factors $Q[S(Q)-1]$ are shown in the figure for better comparison at higher Q values). All features of the experimental curve are well reproduced over the whole Q range. Figures 3(b)–3(e) show the partial radial distribution functions, which give new and complementary information on the atom-atom correlations. It is clear from the figure that the shoulder at the right-hand side of the first peak in the total $G(r)$ in Fig. 2 is really due to Al-Ge and Al-Al correlations. The first peak in these two radial distribution functions is rather broad, with the tail at the right-hand side ex-

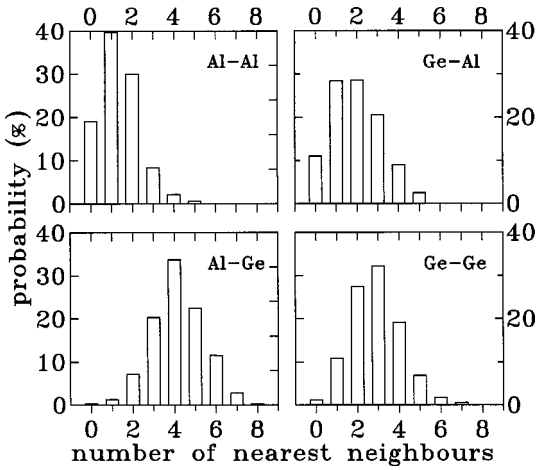

FIG. 4. The distribution of the number of neighbors within the first coordination shell for Al-Al (top, left), Al-Ge (bottom left), Ge-Al (top right), and Ge-Ge (bottom right).

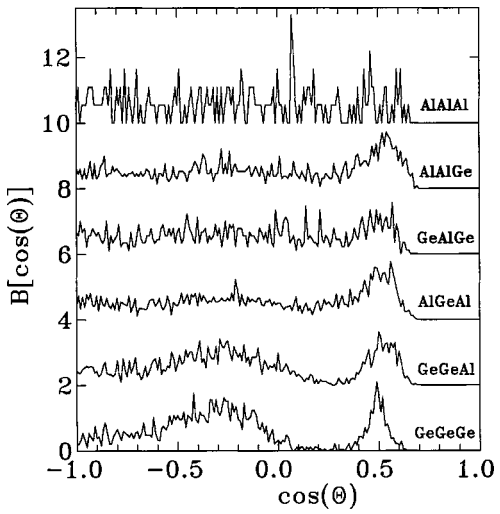

FIG. 5. Distribution of the cosine of the bond angles, $B[\cos(\theta)]$, for Ge-Ge-Ge, Ge-Ge-Al, Al-Ge-Al, Ge-Al-Ge, Al-Al-Ge, and Al-Al-Al, calculated by using the results of the RMC simulations for amorphous $Al_{32}Ge_{68}$.

tending above 3 Å. Very small correlations are seen up to 5.5 Å for Al-Al pairs and up to 7 Å for Al-Ge pairs. As for the Ge-Ge pair-correlation function, it exhibits a very sharp first peak, with a maximum at 2.48 Å, which is slightly larger than the covalent diameter for a Ge atom (2.44 Å), and the first peak is well isolated from the second one. The intensity of the curve between these two peaks is close to zero, which means that the atoms in Ge-Ge pairs are connected by rather well-defined covalent bonds.

The interesting feature of the atomic distribution obtained by RMC calculation should be mentioned. Thus, the smallest distance between the Al-Ge atoms appears to be the shortest interatomic distance in the system [see Figs. 3(c) and 3(e)]. This means that the closest Al-Ge pairs surely cannot be described by a common hard-spheres model.

Using the three-dimensional atomic coordinates obtained, the probability functions for atoms of type *i* having atoms of type *j* as nearest neighbors were calculated. The corresponding curves are shown in Fig. 4. The average coordination numbers (number of atoms in the first coordination sphere of radius 3.1 Å) calculated are: 1.37 for Al-Al, 4.16 for Al-Ge, 1.96 for Ge-Al, and 2.88 for Ge-Ge pairs. One can conclude that most Ge-Ge nearest neighbors do not form tetrahedral units. The more probable elementary unit around a Ge atom consists of 2.88 other (covalently bonded) Ge atoms and 1.96 Al atoms, which means a Ge atom has 4.84 nearest neighbors in average. This is not seen from the analysis of the total radial distribution function $G(r)$ discussed above because it represents the sum of partial $G_{ij}(r)$ weighted by the coefficients, which are small for Al-containing correlations due to the small coherent neutron-scattering cross section for Al atoms, (see Sec. III). The total coordination number for Al atoms (due to Al-Al and Al-Ge correlations) is 5.53 and it was expected to be large due to supposed noncovalent bonding between them. For Al-Al pairs the average coordination number is 1.37. Aluminum atoms are consequently connected mainly in groups of two or three atoms and do not construct a continuous network through the sample—there is no percolation of aluminum atoms in the sample.

It is known that the orientational correlations in disordered structures could be well represented by the distribution of the cosine of the bond angles, $B[\cos(\theta)]$. For this reason the bond-angle distributions for Ge-Ge-Ge, Ge-Ge-Al, Al-Ge-Al, Ge-Al-Ge, Al-Al-Ge, and Al-Al-Al were calculated by using the results of the RMC simulations for amorphous $Al_{32}Ge_{68}$ and the results are shown in Fig. 5. Bonds were defined by neighbors within the first coordination shell ($r < 3.1$ Å). The curve for Al-Al-Al cosine bond-angles distribution shows very poor statistics because, as seen from Fig. 4(a), the probability for Al atom to have two or more other Al atoms as the nearest neighbors is relatively small. The bond-angles distribution for ''ideal'' tetrahedral network should show only one maximum corresponding to the tetrahedral angle $\theta = 109.5°$. Figure 5 clearly shows that Ge-Ge-Ge cosine bond-angles distribution exhibits a broad peak around $\cos(\theta) = -0.3$ (corresponding to $\theta = 107.5°$, which is close to tetrahedral angle) and a sharp peak at $\cos(\theta) \cong 0.5$ (corresponding to $\theta \cong 60°$). These features indicate a presence of large amount of tetrahedral arrangement of the Ge-Ge-Ge atoms in the alloy and, in addition, ''triangular'' configurations of the atoms in amount of about 19% [an integrated area under the peak at $\cos(\theta) \cong 0.5$]. This angle ($\theta = 60°$) is characteristic of close packing in the system, and, actually, the ''triangular'' atomic configurations [corresponding to $\cos(\theta) = 0.5$] are very common for the liquid state of Si and Ge samples.[30] The observed effect correlates well with the results of recent RMC studies[25] of structure of amorphous Ge, Si, and C that have identified a presence of covalent bonding with corresponding local tetrahedral ordering and a rather large portion of ''triangular'' atomic arrangements in these systems. The distribution for Ge-Ge-Al cosine bond angles looks very similar to Ge-Ge-Ge (see Fig. 5), but with a larger amount of ''triangular'' atomic configurations, ~24%. The distributions involving two Al and one Ge atoms do not show a well-defined peak corresponding to tetrahedral atomic arrangement. The peak at $\cos(\theta) \cong 0.5$ for these distributions is rather large, 36% for Al-Al-Ge and 38% for Al-Ge-Al, indicating their ''triangular'' close-packed atomic configurations and, therefore, predominantly nontetrahedral arrangements in these units. The bond-angles

distribution for Ge-Al-Ge has poor-defined structure, which has to be a consequence of their very broad bond-angles distribution.

V. DISCUSSION

It is interesting to compare the $S(Q)$ and $G(r)$ data for the amorphous $Al_{32}Ge_{68}$ alloy studied and for pure amorphous Ge produced by deposition technique.[31] At first sight the spectra appear very similar, but the quantitative values are completely different. The amorphous Ge is less dense ($\rho_0 = 0.03975$ at./Å^3) compared to the $Al_{32}Ge_{68}$ alloy ($\rho_0 = 0.0458$ at./Å^3), but the peaks in the $G(r)$ spectrum in the present study are slightly shifted to larger distances [the position of the first peak in $G(r)$ for amorphous Ge is at 2.463 Å (Ref. 32)]. This results in the principal difference that the first coordination number for amorphous $Al_{32}Ge_{68}$ is 4.5 (with a contribution of only 2.88 due to Ge-Ge correlations) while it is 3.68 for amorphous Ge.

Reference should be made to the recent studies of amorphous Al-Ge alloys by Yvon and coworkers,[32] Degtyareva *et al.*,[33] and Barkalov *et al.*.[34] The authors of Ref. 32 produced two types of amorphous Al-Ge alloy by the pressure-induced solid-state reaction and studied their structure by transmission electron microscopy at ambient conditions. For high-pressure treatments Al-Ge alloys of 20–60 at.% Ge were prepared by mechanical alloying. The state, called amorphous AlGe-I, was produced by applying a pressure between 2.5 and 8 GPa at room temperature and then releasing the pressure to ambient. The stability range of AlGe-I was located within 60–100 at.% Ge interval. Another state, amorphous AlGe-II, was obtained at pressures above 8 GPa. It had a higher density and was described as a metalliclike phase with a coordination number close to 12.

In Ref. 33 energy dispersive x-ray diffraction was applied to study the structural transformations under pressure at room temperature in amorphous $Al_{30}Ge_{70}$ alloy produced by the method described in Ref. 17. Amorphous sample crystallized to the phase with a simple hexagonal structure (γ phase) at pressures between 4.3 and 5.5 GPa. The γ phase was stable up to 47 GPa (similar results were obtained in Ref. 34 for the $Al_{32}Ge_{68}$ amorphous alloy). This is 5 times higher than reported in Ref. 32 pressure of 8 GPa for formation of the amorphous AlGe-II. When the pressure was released the γ phase underwent reverse transformation to the starting amorphous state.[33,34]

Thus, formation of the amorphous state like AlGe-II reported in Ref. 32 was not observed in Refs. 33 and 34. This can be attributed to the different compositions of the starting alloys and also to the different initial states of the samples (the starting material in Ref. 32 was fine mixture of fcc Al and diamond-type Ge prepared by mechanical alloying of the elemental powders). Further *in situ* structure investigations using synchrotron radiation are necessary in order to observe formation of the amorphous AlGe-II under pressure.

The position of the first two halos for AlGe-I observed in the electron-diffraction pattern[32] had values of 1.96 and 3.27 Å^{-1}. The first coincides with the present data but the value for the second peak is smaller than the 3.35 Å^{-1} observed here. In Ref. 32 the diamondlike structure of amorphous AlGe-I was postulated and the nearest-neighbor distance in amorphous AlGe-I was calculated to be about 2.4 Å (compared with 2.48 Å determined in the present investigation from the partial Ge-Ge radial distribution function). So, it seems that the amorphous AlGe-I sample obtained in Ref. 32 has common features with the sample investigated in the present paper.

VI. CONCLUSIONS

It is shown that for the amorphous $Al_{32}Ge_{68}$ alloy produced by heating of the quenched high-pressure phase at ambient pressure the effective coordination number ($n = 4.5$) is appreciably higher than 4, which is characteristic for a tetrahedral coordination. The first peak of the total radial distribution function has a pronounced right-hand shoulder visible up to 3.1 Å. The RMC calculations for amorphous $Al_{32}Ge_{68}$ have shown that the partial radial distribution function for Ge-Ge correlations exhibits a sharp peak at a distance close to the value for the Ge-Ge covalent bond, but Ge atoms do not form a tetrahedral arrangement (the corresponding first coordination number is $n = 2.88$). It was found that the Al-Ge and Al-Al correlations (with total $n = 5.53$) increase the effective coordination number to the observed value of 4.5 and result in the formation of the broad right-hand shoulder of the first peak in the total $G(r)$ function. It was concluded also that aluminum atoms ($n = 1.37$) do not construct a continuous network through the sample.

ACKNOWLEDGMENTS

This work has partly been financed by the CNRS–Russian Academy of Science Collaboration Agreement under Contract No. 4069, by the Royal Swedish Academy under Contract No. 1454, by the RFBR Grants No. 96-15-96806 and No. 99-02-17007, and by the Grant No. 34-1997 for young scientists from the Russian Academy of Sciences. The authors would like to thank ISIS for the provision of neutron beam facilities. One of the authors (O.I.B) thanks the Alexander von Humboldt Foundation for support.

*Author to whom correspondence should be addressed; present address: Fachbereich Physik, Universität-GH-Pderborn, D-33095 Paderborn, Germany.

[1] E. G. Ponyatovsky and O. I. Barkalov, Mater. Sci. Eng., A **133**, 726 (1991).

[2] E. G. Ponyatovsky and O. I. Barkalov, Mater. Sci. Rep. **8**, 147 (1992).

[3] V. E. Antonov, A. E. Arakelyan, O. I. Barkalov, A. F. Gurov, E. G. Ponyatovsky, V. I. Rashupkin, and V. M. Teplinsky, J. Alloys Compd. **194**, 279 (1993).

[4] V. E. Antonov, O. I. Barkalov, and E. G. Ponyatovsky, J. Non-Cryst. Solids **192&193**, 443 (1995).

[5] O. I. Barkalov, A. I. Kolesnikov, E. G. Ponyatovsky, U. Dahlborg, R. Delaplane, and A. Wannberg, J. Non-Cryst. Solids **176**, 263 (1994).

[6] O. I. Barkalov, A. I. Kolesnikov, V. E. Antonov, E. G. Ponyatovsky, U. Dahlborg, M. Dahlborg, and A. C. Hannon, Phys. Status Solidi B **198**, 491 (1996).

[7] U. Dahlborg, M. Calvo-Dahlborg, A. I. Kolesnikov, O. I. Barkalov, V. E. Antonov, and E. G. Ponyatovsky, Mater. Sci. Eng., A **226**, 448 (1997).
[8] M. Calvo-Dahlborg, U. Dahlborg, A. I. Kolesnikov, O. I. Barkalov, E. G. Ponyatovsky, and A. C. Hannon, J. Non-Cryst. Solids **244**, 250 (1999).
[9] A. S. Aronin, O. I. Barkalov, and E. G. Ponyatovsky, J. Non-Cryst. Solids **189**, 138 (1995).
[10] O. I. Barkalov, A. S. Aronin, G. E. Abrosimova, and E. G. Ponyatovsky, J. Non-Cryst. Solids **202**, 266 (1996).
[11] M. Hansen, *Constitution of Binary Alloys* (McGraw-Hill, New York, 1958).
[12] U. Koster, Z. Metallkd. **63**, 472 (1972).
[13] M. J. Kaufman and H. L. Fraser, Acta Metall. **33**, 191 (1985).
[14] S. N. Ojha, Z. Metallkd. **82**, 41 (1991).
[15] L. T. Laoui and M. J. Kaufman, Metall. Trans. A **22**, 2141 (1991).
[16] O. I. Barkalov and G. V. Chipenko, in *Proceedings of the XI AIRAPT International Conference, Kiev, 1987*, edited by N. V. Novikov (Naukova Dumka, Kiev, 1989), Vol. 1, p. 270.
[17] O. I. Barkalov, I. T. Belash, V. F. Degtyareva, and E. G. Ponyatovsky, Fiz. Tverd. Tela (Leningrad) **29**, 1975 (1987) [Sov. Phys. Solid State **29**, 1144 (1987)].
[18] *ISIS Experimental Facilities*, edited by B. Boland and S. Whapham (Rutherford-Appleton Laboratory, UK, 1992).
[19] A. K. Soper, W. S. Howells, and A. C. Hannon, *ATLAS Analysis of Time-of-Flight Diffraction Data from Liquid and Amorphous Samples* (Rutherford-Appleton Laboratory, UK, 1989).
[20] N. W. Ashcroft and D. C. Langreth, Phys. Rev. **159**, 500 (1967).
[21] R. L. McGreevy and L. Pusztai, Mol. Simul. **1**, 359 (1988).
[22] D. A. Keen and R. L. McGreevy, Nature (London) **344**, 423 (1990).
[23] R. L. McGreevy, Nucl. Instrum. Methods Phys. Res. A **354**, 1 (1995).
[24] S. Kugler, L. Pusztai, L. Rosta, P. Chieux, and R. Bellissent, Phys. Rev. B **48**, 7685 (1993).
[25] O. Gereben and L. Pusztai, Phys. Rev. B **50**, 14 136 (1994).
[26] J. K. Walters and R. J. Newport, Phys. Rev. B **53**, 2405 (1996).
[27] K. W. R. Gilkes, P. H. Gaskell, and J. Robertson, Phys. Rev. B **51**, 12 303 (1995).
[28] J. K. Walters, K. W. R. Gilkes, J. D. Wicks, and R. J. Newport, Phys. Rev. B **58**, 8267 (1998).
[29] B. O'Malley, I. Snook, and D. McCulloch, Phys. Rev. B **57**, 14 148 (1998).
[30] V. Petkov and G. Yunchov, J. Phys.: Condens. Matter **6**, 10 885 (1994).
[31] G. Etherington, A. C. Wright, J. T. Wenzel, J. C. Dore, J. H. Clarke, and R. N. Sinclair, J. Non-Cryst. Solids **48**, 265 (1982).
[32] P. J. Yvon, R. B. Schwarz, D. Schiferl, and W. L. Johnson, Philos. Mag. Lett. **72**, 167 (1995).
[33] V. F. Degtyareva, F. Porsch, E. G. Ponyatovsky, and W. B. Holzapfel, Phys. Rev. B **53**, 8337 (1996).
[34] O. I. Barkalov, A. Schiwek, and W. B. Holzapfel, in *HASYLAB Annual Report 1998*, edited by W. Laasch, G. Materlik, J. R. Schneider, and H. Schulte-Schrepping (HASYLAB, Hamburg, 1998), Part 1, p. 689.